A METHOD FOR EVALUATING EXPERIMENTAL DATA IN BUBBLE DYNAMICS STUDIES*)

K. Vokurka**)

Department of Physics, Faculty of Electrical Engineering, Czech Technical University, Suchbátarova 2, 166 27 Praha 6, Czechoslovakia

Free oscillations of gas bubbles in compressible liquids are analysed. Gilmore's model is used to compute the scaling and independent functions that make it possible to evaluate experimental data. The method is illustrated by examples. A possibility of using the scaling functions for determination of the bubble pulse spectrum is also demonstrated.

1. INTRODUCTION

In previous works [1–3] we have suggested a use of the scaling and independent functions to evaluate the unknown parameters of bubbles freely oscillating in liquids. It has also been shown that Rayleigh's model, thanks to its simplicity, enables one to gain a necessary qualitative insight into the bubble behaviour with relative ease. However, due to the assumption of liquid incompressibility the quantitative results obtained with Rayleigh's model are valid only for moderate amplitudes of bubble oscillations [4].

In this paper we want to extend the analysis of the bubble behaviour to cover the compressible liquids so that the method developed in [1–3] can be used to evaluate the experimental data for a much wider range of amplitudes of bubble oscillations. For this purpose the scaling and independent functions are calculated here with the use of Gilmore's model [4].

Though the method can be applied to bubbles of any size, to take an advantage of the scaling law [5], only the scaling, i.e. the medium-sized bubbles, will be considered here.

In order to illustrate the potentialities of the method, experimental data found in the literature will be used to determine the unknown parameters in particular cases of the explosion and spark generated bubbles.

2. FORMULATION

Let us consider a spherical gas bubble situated in a liquid far from boundaries and freely oscillating. In this work the method of the bubble excitation for free oscillations [6] will be immaterial and the analysis starts at the moment the bubble attains a maximum radius R_M. We shall be interested in the processes associated with the bubble wall motion between two successive radius maxima, e.g. between

*) This work is taken from the author's Ph. D. dissertation [25] and in a shortened form it was also presented at the seminar on cavitation [26].

**) Present address: *Department of Research and Development, LIAZ n. p., tř. V. Kopeckého 400, 466 05 Jablonec n. N., Czechoslovakia.*

R_{M1} and R_{M2}. Evidently, the analysis can easily be extended to include any two successive maxima. Hence, to simplify the notation, the digits denoting the oscillation period will often be omitted from the subscripts.

An example of the bubble wall motion is given in fig. 1. A corresponding energy equation for the bubble can be written in the compression system as [1–3]

$$\Delta E_p = \Delta E_i + E_k + \Delta E_d \,. \tag{1}$$

Here E_k is the liquid kinetic energy, and ΔE_d the dissipated energy. The change in the potential energy of the bubble, ΔE_p, equals

$$\Delta E_p = \tfrac{4}{3}\pi p_\infty R_{M1}^3 \left[1 - \left(\frac{R}{R_{M1}}\right)^3\right], \tag{2}$$

and the change in the internal energy of the gas, ΔE_i, can be written as

$$\Delta E_i = \tfrac{4}{3}\pi \frac{1}{\gamma - 1} P_{m1} R_{M1}^3 \left[\left(\frac{R}{R_{M1}}\right)^{-3(\gamma-1)} - 1\right]. \tag{3}$$

Here p_∞ is the pressure in the liquid at a large distance from the bubble, γ is the ratio of the specific heats, and P_{m1} is the pressure at the bubble wall when $R = R_{M1}$.

An oscillating bubble radiates pressure waves into the surrounding liquid. A wave radiated between two successive radius maxima is usually called the bubble pulse [7–9]. The form of the bubble pulse is schematically shown in fig. 2.

Let us denote the acoustic energy radiated by the bubble in the time interval from t_a to t_b by ΔE_a and the acoustic energy passing through a sphere of a radius $r \gg R_{M1}$ by $\Delta E'_a$ (thanks to the propagation losses $\Delta E'_a < \Delta E_a$). Then we can write

$$\Delta E'_a = 4\pi r^2 F \,, \tag{4}$$

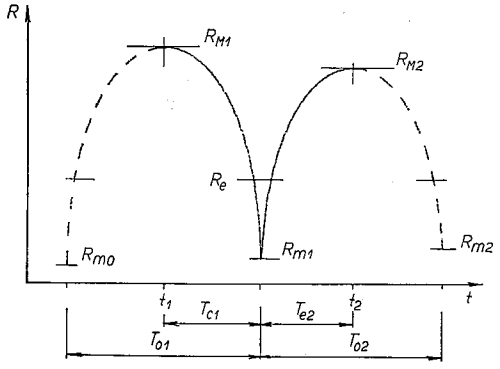

Fig. 1. Radius of the bubble, R, as a function of time, t.

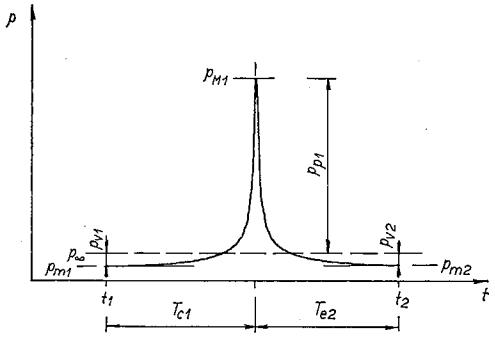

Fig. 2. Pressure-time curve for a bubble pulse.

where F is the acoustic energy flux, which equals [8, 9]

$$F = \frac{1}{\varrho_\infty c_\infty} \int_{t_a}^{t_b} p_a^2 \, dt \,. \tag{5}$$

Here c_∞ is the velocity of sound in an undisturbed liquid, ϱ_∞ is the liquid density at a large distance from the bubble, and $p_a = p - p_\infty$ is the acoustic pressure in the wave at the point r. For moderate intensities of the bubble oscillations p_a can be conveniently computed from a simple formula that was given in work [1].

In [1] the effective pulse width, ϑ, was defined by the relation

$$\vartheta = \frac{1}{p_p^2} \int_{t_1}^{t_2} p_a^2 \, \mathrm{d}t \,, \tag{6}$$

where p_p is the peak acoustic pressure in the bubble pulse and t_1, t_2 correspond to two successive moments at which the valley pressures, p_v, occur in the wave (fig. 2).

Finally let us define the damping factor, α_1, for the wall motion between R_{M1} and R_{M2} as

$$\alpha_1 = \frac{R_{M2}}{R_{M1}} \,. \tag{7}$$

For further work it is convenient to introduce the compression non-dimensional variables [1, 6]:

$$t_z = \frac{t}{R_{M1}\sqrt{\dfrac{\varrho_\infty}{p_\infty}}}, \quad E_z = \frac{E}{E_{pM1}}, \quad Z = \frac{R}{R_{M1}}, \quad P^* = \frac{P}{p_\infty},$$

where $E_{pM1} = \frac{4}{3}\pi p_\infty R_{M1}^3$.

Assuming that $E_k \doteq 0$ for $R = R_{M1}$ and $R = R_{M2}$, the non-dimensional energy dissipated between R_{M1} and R_{M2} can be determined from (1), (2), (3), and (7) as

$$\Delta E_{zd1} = \Delta E_{zp1} - \Delta E_{zi1} = 1 - \alpha_1^3 - \frac{1}{\gamma - 1} P_{m1}^* \left[\alpha_1^{-3(\gamma-1)} - 1\right] . \tag{8}$$

For intensively oscillating bubbles the term ΔE_{zi1} is small in comparison with ΔE_{zp1} and therefore can be neglected. We obtain a simple relation

$$\Delta E_{zd1} \doteq 1 - \alpha_1^3 \,, \tag{9}$$

often used in the literature [7–9]. For linear and weakly non-linear oscillations, on the other hand, the terms ΔE_{zp1} and ΔE_{zi1} are comparable and hence the use of eq. (8) may lead to erroneous results. It may be then better to determine the dissipated energy by some other method, e.g. from the effective pulse width.

Combining eqs. (4) to (6) and putting $t_1 = t_a$, $t_2 = t_b$, we can express the non-dimensional acoustic energy in terms of p_{zp} and ϑ_z as

$$\Delta E'_{za1} = \frac{3}{c^*_\infty} \vartheta_{z1} p^2_{zp1} . \tag{10}$$

The non-dimensional quantities occurring in (10) are defined in the following way [1, 4]:

$$c^*_\infty = c_\infty \sqrt{\frac{\varrho_\infty}{p_\infty}} , \tag{11}$$

$$\vartheta_{z1} = \frac{\vartheta_1}{R_{M1} \sqrt{\frac{\varrho_\infty}{p_\infty}}} , \tag{12}$$

$$p_{zp1} = \left(\frac{p_{M1}}{p_\infty} - 1 \right) \frac{r}{R_{M1}} = \frac{p_{p1}}{p_\infty} \frac{r}{R_{M1}} , \tag{13}$$

and the non-dimensional form of eq. (6) is

$$\vartheta_z = \frac{1}{p^2_{zp}} \int_{t_{z1}}^{t_{z2}} p_z^2 \, \mathrm{d}t_z . \tag{14}$$

Let us now define the coefficient of acoustic radiation efficiency

$$\varkappa = \frac{\Delta E_a}{\Delta E_d} , \tag{15}$$

and the coefficient of acoustic losses during propagation of the wave from the bubble wall to a point r

$$\mu = \frac{\Delta E'_a}{\Delta E_a} . \tag{16}$$

In a real environment, evidently, $0 < \varkappa, \mu < 1$. In this work, however, we shall assume that $\varkappa, \mu = 1$. Then $\Delta E'_a = \Delta E_a = \Delta E_d$ and we obtain from eq. (10)

$$\vartheta_{z1} = \frac{c^*_\infty}{3} \frac{\Delta E_{zd1}}{p^2_{zp1}} . \tag{17}$$

Hence ϑ_z can be computed in two ways. For moderate intensities of the buble oscillations eq. (14) gives good results. This is also the only method that can be used for evaluation of experimental data and in the theory of non-scaling bubbles. On the other hand, for violent bubble oscillations, eqs. (9) and (17) are usually more economical with respect to the machine time and one does not need to know the form of p_z in this case.

Finally, the peak pressure, p_{zp1}, can be determined from a relation [1]

$$p_{zp1} = (P^*_{M1} - 1) Z_{m1} = (P^*_{m1} Z^{-3\gamma}_{m1} - 1) Z_{m1} . \tag{18}$$

Let us note that relations (17) and (18) are valid only in the framework of linear acoustics.

In experiments the damping factor, α_1, is often approximated by the ratio of the times of two successive oscillations. Let us determine the error introduced by this approximation. Denoting

$$\beta_1 = \frac{T_{o2}}{T_{o1}}, \tag{19}$$

and using the definition formula for T_{zc} ($T_o \doteq 2T_c$, T_o is the time of the bubble oscillation)

$$T_{zc} = \frac{T_c}{R_M \sqrt{\frac{\varrho_\infty}{p_\infty}}}, \tag{20}$$

we may evaluate the ratio T_{zo1}/T_{zo2}. We find that

$$\frac{T_{zo1}}{T_{zo2}} = \frac{T_{o1} R_{M2}}{T_{o2} R_{M1}} = \frac{\alpha_1}{\beta_1}.$$

As it always holds that $A_1 > A_2$, it follows then that $T_{zc2} > T_{zc1}$ and $T_{zo2} > T_{zo1}$ (cf. fig. 4) and we thus obtain from the above equation an important inequality

$$\beta_1 > \alpha_1 .$$

However, computations show that the actual difference between α and β is small for all amplitudes of interest (typically $\alpha/\beta \doteq 0{\cdot}98 - 0{\cdot}99$).

3. BUBBLE MODEL

All computations presented in this paper have been done with Gilmore's model of a scaling bubble. In this model the equation of motion has the form [4]

$$\ddot{R}R\left(1 - \frac{\dot{R}}{C}\right) + \tfrac{3}{2}\dot{R}^2\left(1 - \frac{1}{3}\frac{\dot{R}}{C}\right) = H\left(1 + \frac{\dot{R}}{C}\right) + \frac{R}{C}\dot{H}\left(1 - \frac{\dot{R}}{C}\right), \tag{21}$$

where C is the velocity of sound in the liquid at the bubble wall

$$C = c_\infty \left(\frac{P + B}{p_\infty + B}\right)^{(n-1)/2n}, \tag{22}$$

H is the enthalpy difference between the liquid at pressures P and p_∞

$$H = \frac{1}{\varrho_\infty}\frac{n}{n-1}(p_\infty + B)\left[\left(\frac{P + B}{p_\infty + B}\right)^{(n-1)/n} - 1\right], \tag{23}$$

and B and n are constants in the Tait equation of state for the liquid. The dots denote differentiation with respect to time. The initial conditions of eq. (21) are $R(0) = R_{M1}$ and $\dot{R}(0) = 0$. Finally, the pressure at the bubble wall, P, is assumed

to vary as

$$P = P_{m1}\left(\frac{R}{R_{M1}}\right)^{-3\gamma}. \tag{24}$$

After normalization of these equations we obtain

$$\ddot{Z}Z\left(1-\frac{\dot{Z}}{C^*}\right)+\tfrac{3}{2}\dot{Z}^2\left(1-\frac{1}{3}\frac{\dot{Z}}{C^*}\right)=H^*\left(1+\frac{\dot{Z}}{C^*}\right)+\frac{Z}{C^*}\dot{H}^*\left(1-\frac{\dot{Z}}{C^*}\right), \tag{25}$$

$$C^* = c_\infty^*\left(\frac{P^*+B^*}{1+B^*}\right)^{(n-1)/2n}, \tag{26}$$

$$H^* = \frac{n}{n-1}(1+B^*)\left[\left(\frac{P^*+B^*}{1+B^*}\right)^{(n-1)/n}-1\right], \tag{27}$$

$$P^* = P_{m1}^* Z^{-3\gamma}, \tag{28}$$

with the initial conditions $Z(0) = 1$ and $\dot{Z}(0) = 0$. Here $B^* = B/p_\infty$.

The intensity of the bubble oscillations will be described by a non-linear amplitude $A_1 = R_{M1}/R_e$, where R_e is the equilibrium radius [1, 6]. Then the minimum pressure, P_{m1}^*, can be expressed as [1]

$$P_{m1}^* = A_1^{-3\gamma}. \tag{29}$$

With the exception of an example given in section 5 the computations have been done for the following values of the physical constants (water under ordinary laboratory conditions):

$$p_\infty = 100\ \text{kPa}, \quad \varrho_\infty = 10^3\ \text{kg m}^{-3}, \quad c_\infty = 1450\ \text{m s}^{-1},$$
$$B = 300\ \text{MPa}, \quad n = 7.$$

4. SCALING AND INDEPENDENT FUNCTIONS

The method to be discussed is based on a comparison of measured and computed values of selected quantities. These selected quantities are the minimum bubble radius, Z_m, the time of bubble compression, T_{zc}, the peak pulse pressure, p_{zp}, the effective width of the bubble pulse, ϑ_z, the dissipated energy, ΔE_{zd}, the damping factor, α, and the maximum wall velocity, $\dot{Z}_{max}$. The functional dependences of these quantities on the amplitude, A, and adiabatic exponent, γ, were denoted as the scaling functions (Z_m, T_{zp}, p_{zp}, ϑ_z, and ΔE_{zd}) and the independent functions (α, and $\dot{Z}_{max}$) [2].

For small amplitudes ($A \leqq 2$) the scaling and independent functions were computed in [2]. In this section we shall present results of computations of these functions for amplitudes as large as $A \leqq 4$ (the scaling functions) and $A \leqq 10$ (the damping factor). In fact, all the computations were performed for the amplitudes $A \leqq 10$,

but after examination of the available experimental data it was decided to display the scaling functions just for the limited range of amplitudes mentioned.

The scaling functions $Z_m = Z_m(A, \gamma)$ and $T_{zc} = T_{zc}(A, \gamma)$ have been determined by direct integration of eq. (25) and are displayed in figs. 3 and 4. In the case of the violently oscillating bubbles experimental measurements of Z_m encounter great

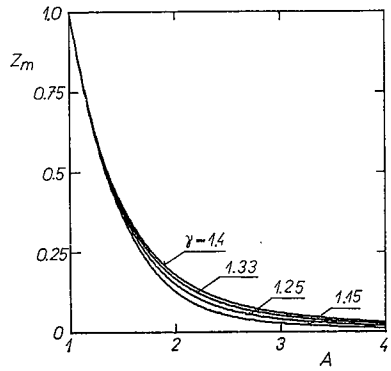

Fig. 3. Scaling function $Z_m(A, \gamma)$.

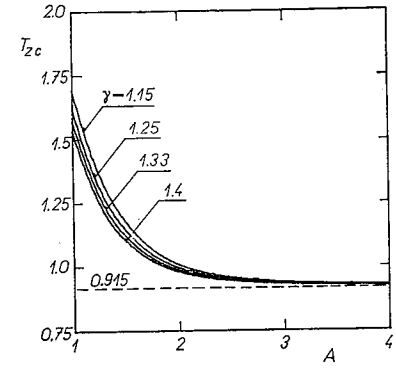

Fig. 4. Scaling function $T_{zc}(A, \gamma)$.

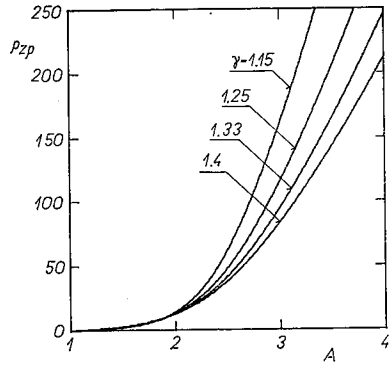

Fig. 5. Scaling function $p_{zp}(A, \gamma)$.

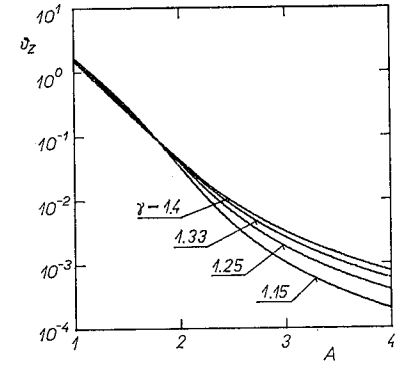

Fig. 6. Scaling function $\vartheta_z(A, \gamma)$.

difficulties (see, e.g. [7, 10]); however, it is of great interest because it serves as a basis for the determination of many other related quantities. The quantity T_{zc} is of great practical importance because it can be easily measured. It also enables one to determine the bubble size, R_M, just from the measurement in the time domain. As can be seen in fig. 4, the function $T_{zc}(A, \gamma)$ approaches the asymptotic value of 0·915 very quickly. For example, for $A \geqq 3$ the deviation of T_{zc} from the value 0·915 represents just a few per cent ($<2{\cdot}7\%$).

The scaling functions $p_{zp} = p_{zp}(A, \gamma)$ and $\vartheta_z = \vartheta_z(A, \gamma)$ are displayed in figs. 5 and 6. The function p_{zp} was determined from eq. (18) and the function ϑ_z both from eq. (14) (small A) and eqs. (9), (17) (large A). As noted in section 2, eqs. (17) and (18)

assume acoustic propagation of the pressure waves and therefore can be used only for moderate amplitudes of the bubble oscillations. However, no attempt was undertaken here to determine the amplitudes, A, for which the finite-amplitude effects in radiated waves become important.

The scaling function $\Delta E_{zd} = \Delta E_{zd}(A, \gamma)$ is given in fig. 7. As in the case of ϑ_z, the function ΔE_{zd} was calculated both from eq. (10) (small A) and eq. (9) (large A).

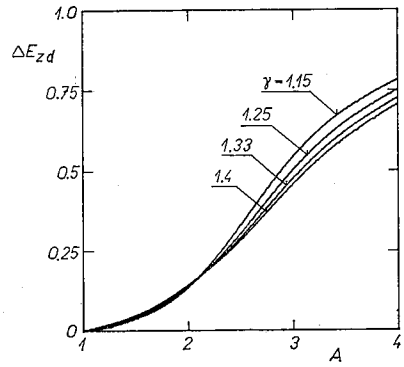

Fig. 7. Scaling function $\Delta E_{zd}(A, \gamma)$.

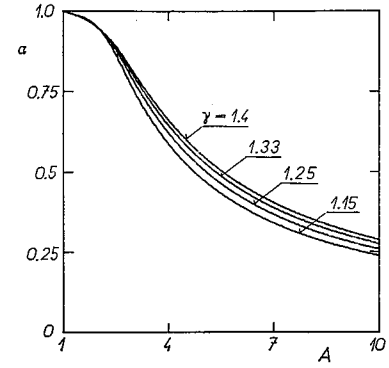

Fig. 8. Independent function $\alpha(A, \gamma)$.

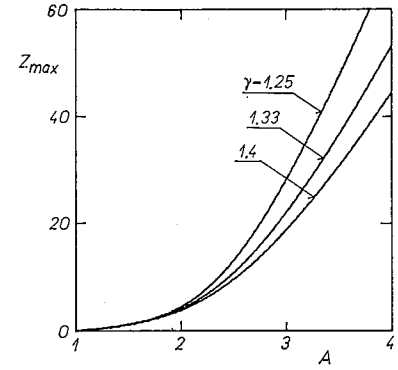

Fig. 9. Independent function $\dot{Z}_{max}(A, \gamma)$.

The calculated independent functions $\alpha = \alpha(A, \gamma)$ and $\dot{Z}_{max} = \dot{Z}_{max}(A, \gamma)$ are displayed in figs. 8 and 9. The functions α and $\dot{Z}_{max}$ were determined by direct integration of eq. (25). The quantity α is very useful for the evaluation of experiments, because apart from the bubble size, R_M, it often represents the only available information given in the literature. Though α was displayed for values of A as great as 10, it should be noted here that the area of the bubble model validity is limited to moderate amplitudes [4, 11]. Hence, the results obtained for larger A should be considered as a first approximation only. The quantity $\dot{Z}_{max}$ was included because it is occasionally measured in experiments by photographic methods. It can also be used to check the model validity [11].

From the definition of the damping factor, α_1, it follows that

$$A_2 = \alpha_1 A_1 \,. \tag{30}$$

Hence, there is no sense in integrating eq. (25) behind R_{M2}, because once the scaling and independent functions are determined for the first bubble oscillation and the first bubble pulse, we have sufficient information at our disposal to determine the bubble behaviour at any further time. For example, for given A_1 we can determine from fig. 8 the corresponding value of α_1 and then from eq. (30) the value of A_2. By repeating this procedure we can find the amplitude for any further bubble oscillation. And when the amplitude is known, the corresponding scaling and independent quantities can always be determined from figs. 3 to 9.

What has just been said does not, of course, apply for models which take the previous bubble history into account, such as the models considering the effect of gravity, gas diffusion, etc. In these models, for any new oscillation new results will be obtained. But let us note here that such models are only rarely used at present.

5. EXAMPLES OF APPLICATIONS

As said above the method for evaluating the unknown bubble parameters is based on the comparison of the measured data with scaling and independent functions computed with the aid of a suitable theoretical model. In a general case the functions Z_m, T_{zc}, p_{zp}, ϑ_z, ΔE_{zd}, α, and $\dot{Z}_{max}$ are general surfaces above the $R_M - A$ plane (the bubble map). However, as the scaling law asserts [5], for scaling bubbles the analysis is substantially simplified. The simplification consists in the fact that the quantities mentioned are either independent of the bubble size (the independent quantities) or they are in the dimensional form linear functions of the bubble size (the scaling quantities). The quantity ΔE_d is an exception because it grows as R_M^3.

A freely oscillating bubble is described by its size, R_M, and amplitude of oscillations, A. Whereas the direct measurement of R_M usually represents no serious problem, the situation is different as far as A is concerned. The reason is that with the exception of linear oscillations and excitation in the equilibrium system there is no direct method available to measure A. Hence, indirect methods, such as the method of the scaling and independent functions, must be used.

In theory, to determine these two parameters we need to measure two quantities, e.g. T_{zc} and p_{zp}. In practice, however, because $\varkappa, \mu \neq 1$, we shall encounter serious discrepancies when comparing the measured data with a theoretical model. Then, a measurement of as many quantities as possible is necessary to obtain a more complete picture.

As far as the time domain measurements are concerned, there is quite good agreement between the theory and experiment. For example, Rayleigh's time for the bubble collapse, $T_{zc} = 0{\cdot}915$, agrees well with the measured data (see, e.g. fig. 11 in [10]). The same is true for Minnaeret's frequency of the free linear oscillations

$\omega_{x0} = \pi/(3\gamma)^{1/2}$ [12]. Encouraging experimental results have also been reported recently on measurement of the polytropic exponent by Crum [13]. However, as we shall see later, the situation is completely different as far as the energies are concerned.

The task of assessing the validity of the bubble models and determining the amplitude, A, is also complicated at present by the fact that up to now only few experimental works, in which a sufficient number of quantities were measured simultaneously, have been published, and that often the experiments are performed with the non-scaling bubbles.

In fact, we know only one experimental work [8, 9], where relatively extensive data were collected. In this work it was found that (in the following, G is the weight of the explosive used and h the depth of explosions)

(31) $$R_{M1} = 12{\cdot}6G^{1/3}/h_o^{1/3}, \quad [\text{ft, lb, ft}]$$
$$= 3{\cdot}36G^{1/3}/h_o^{1/3}, \quad [\text{m, kg, m}]$$

(32) $$R_{M2} = 8{\cdot}5G^{1/3}/h_o^{1/3}, \quad [\text{ft, lb, ft}]$$
$$= 2{\cdot}27G^{1/3}/h_o^{1/3}, \quad [\text{m, kg, m}]$$

(33) $$T_{o1} = 4{\cdot}36G^{1/3}/h_o^{5/6}, \quad [\text{s, lb, ft}]$$
$$= 2{\cdot}11G^{1/3}/h_o^{5/6}, \quad [\text{s, kg, m}]$$

(34) $$T_{o2} = 3{\cdot}06G^{1/3}/h_o^{5/6}, \quad [\text{s, lb, ft}]$$
$$= 1{\cdot}48G^{1/3}/h_o^{5/6}, \quad [\text{s, kg, m}]$$

where

(35) $$h_o = h + 33, \quad [\text{ft}]$$
$$= h + 10{\cdot}06. \quad [\text{m}]$$

Further it was determined that

(36) $$p_{p1} = 1200, \quad [\text{lb in}^{-2}]$$
$$= 82{\cdot}7 \times 10^5, \quad [\text{Pa}]$$

(37) $$p_{p2} = 250, \quad [\text{lb in}^{-2}]$$
$$= 17{\cdot}3 \times 10^5, \quad [\text{Pa}]$$

(38) $$F_1 = 139G^{1/3}, \quad [\text{in lb in}^{-2}, \text{lb}]$$
$$= 31{\cdot}7 \times 10^3 G^{1/3}, \quad [\text{kg s}^{-2}, \text{kg}]$$

(39) $$F_2 = 16{\cdot}8G^{1/3}, \quad [\text{in lb in}^{-2}, \text{lb}]$$
$$= 3{\cdot}83 \times 10^3 G^{1/3}, \quad [\text{kg s}^{-2}, \text{kg}]$$

where the quantities p_{p1}, p_{p2}, F_1, and F_2 were measured at the distance from the

charge centre equal to

$$r = 2{\cdot}84G^{1/3}\,, \quad [\text{ft, lb}] \tag{40}$$
$$= 1{\cdot}13G^{1/3}\,. \quad [\text{m, kg}]$$

Finally, it was found that

$$\gamma = 1{\cdot}25\,,$$
$$\alpha_1 = 0{\cdot}68\,,$$
$$\beta_1 = 0{\cdot}70\,,$$
$$\beta_2 = 0{\cdot}82\,.$$

The measurements were done at a depth $h = 500$ ft (152·4 m), so that $p_\infty = 1{\cdot}62$ MPa.

After substituting $h = 152{\cdot}4$ m into eqs. (31) to (34) and replacing in the remaining expressions $G^{1/3}$ with R_{M1} and R_{M2} (using eqs. (31) and (32), respectively) we may substitute eqs. (33), (34), and (36) to (40) into formulae (4), (13), (17), and (20). The values of the non-dimensional quantities thus obtained are given in table I. As the ambient pressure, p_∞, in this example substantially differs from the "ordinary" value $p_\infty = 100$ kPa, the graphs determined in the preceding section unfortunately cannot be used now. New functions computed specially for $p_\infty = 1{\cdot}62$ MPa and $\gamma = 1{\cdot}25$ are displayed in figs. 10 to 12. The values of the amplitudes A_1 and A_2 determined from these graphs are given in the second column of table I. For comparison results found from the scaling functions computed with Rayleigh's model [2] are given in the third column of table I.

The puzzling feature occurring in table I is an enormous scatter in values A_1 and A_2 (especially in connection with the damping factors α_1 and α_2). The reason

Table I

To the example: The values of experimentally determined non-dimensional quantities associated with the first and second bubble oscillation and the first and second bubble pulse (first column) and the corresponding theoretical amplitudes determined from figs. 10 to 12 (second column) and from figs. II-8 to II-10 in [2] (third column).

$T_{zc1} = 0{\cdot}995$	$A_1 = 2{\cdot}02$	$A_1 = 2{\cdot}0$
$p_{zp1} = 9{\cdot}5$	$A_1 = 2{\cdot}05$	$A_1 = 1{\cdot}85$
$\vartheta_{z1} = 0{\cdot}17$	$A_1 = 2{\cdot}1$	$A_1 = 1{\cdot}98$
$\Delta E_{za1} = 0{\cdot}32$	$A_1 = 1{\cdot}9$	
$\alpha_1 = 0{\cdot}68$	$A_1 = 2{\cdot}7$	
$T_{zc2} = 1{\cdot}013$	$A_2 = 1{\cdot}92$	$A_2 = 1{\cdot}88$
$p_{zp2} = 2{\cdot}91$	$A_2 = 1{\cdot}59$	$A_2 = 1{\cdot}5$
$\vartheta_{z2} = 0{\cdot}685$	$A_2 = 1{\cdot}67$	$A_2 = 1{\cdot}62$
$\Delta E_{za2} = 0{\cdot}12$	$A_2 = 1{\cdot}45$	
$\alpha_2 \doteq 0{\cdot}98\beta_2 = 0{\cdot}80$	$A_2 = 2{\cdot}2$	

for this scatter is, apparently, some dissipative mechanism not accounted for in the theoretical model. Indeed, whereas the first bubble pulse carries away approximately 32% of E_{pM1}, the energy dissipated between R_{M1} and R_{M2} accounts for $\Delta E_{zd1} \doteq \doteq 1 - \alpha_1^3 = 68\%$ of E_{pM1}. Similarly, the second bubble pulse carries away 12% of E_{pM2} but the dissipated energy accounts for $\Delta E_{zd2} \doteq 1 - (0{\cdot}98\beta_2)^3 = 49\%$.

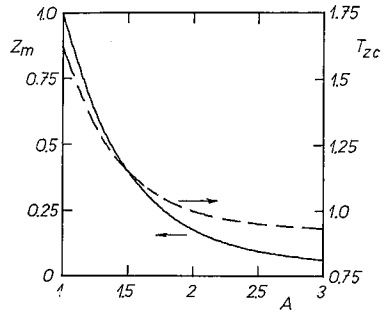

Fig. 10. To the example: Scaling functions Z_m (———) and T_{zc} (— — —) for the ambient pressure $p_\infty = 1{\cdot}62$ MPa and $\gamma = 1{\cdot}25$.

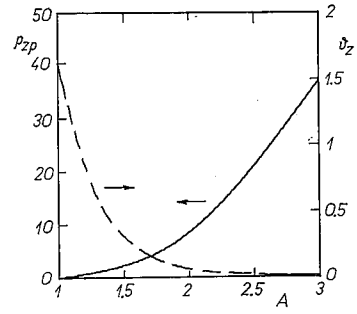

Fig. 11. To the example: Scaling functions p_{zp} (———) and ϑ_z (— — —) for the ambient pressure $p_\infty = 1{\cdot}62$ MPa and $\gamma = 1{\cdot}25$.

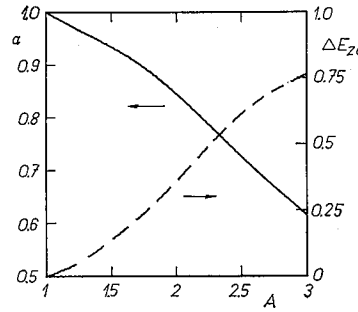

Fig. 12. To the example: Scaling and idependent functions α (———) and ΔE_{zd} (— — — —) for the ambient pressure $p_\infty = 1{\cdot}62$ MPa and $\gamma = 1{\cdot}25$.

These facts have been known more than 40 years [7–9], but, strangely enough, they do not seem to worry many workers in the field of bubble dynamics.

In closing let us verify whether the bubbles generated in the considered example were the scaling bubbles. The charge weights used in the experiments ranged from 0·505 to 12·01 lb (0·23 to 5·45 kg) so that the bubble sizes, R_M, ranged from 0·38 to 1·08 m. In [3, 5] the limiting bubble size for amplitude $A = 2$ and the ambient pressure $p_\infty = 100$ kPa was found to be $R'_M \doteq 0{\cdot}1$ m. Then from the principle of similarity [5] it follows that for the ambient pressure increased by a factor 16·2, the limiting bubble size is also increased by the same factor and hence of $R'_M \doteq 1{\cdot}6$ m, which is well above the bubble sizes used. This is certainly no new result as the validity of the scaling law was verified experimentally first of all [8, 9], but for us it represents an important check of the theory [3, 5].

As a second example let us briefly evaluate data published by Mellen [14]. Mellen worked with spark generated bubbles and measured the time of the first oscillation, T_{o1}, and the peak pressure in the first bubble pulse, p_{p1}, at a distance $r = 1$ m (the actual measurements were done at $r = 0{\cdot}5$ m, but the published data were converted for $r = 1$ m). As the spark bubbles oscillate very violently, the time of the first bubble compression can be assumed to be equal to $T_{zc1} = 0{\cdot}915$ (cf. fig. 4). Then assuming that $T_{o1} \doteq 2T_{c1}$ we obtain from (20) for ordinary laboratory conditions a relation $R_{M1} \doteq T_{o1}/0{\cdot}183$, which enables one to determine the bubble size just from a time domain measurement.

The measured peak pressures, p_{p1}, *vs* bubble sizes, R_{M1}, were reproduced in [5], where it was also shown that in the range of the scaling bubbles the variation of p_{p1} with R_{M1} can be approximated by a straight line in the form $p_{p1} = C_1 R_{M1}$, where $C_1 = 1{\cdot}67 \times 10^7$ Pa m^{-1}. Substituting this equation into the definition formula (13) we find that for $p_\infty = 100$ kPa and $r = 1$ m the non-dimensional peak pressure is $p_{zp1} = 167$.

Let us now compare the two examples discussed. The bubbles generated by underwater explosions are typical gas bubbles which oscillate with moderate amplitudes (e.g. the value of $p_{zp1} = 9{\cdot}5$ gives $A_1 = 2{\cdot}05$). On the other hand, the spark generated bubbles are vapour bubbles oscillating very violently, the pressure p_{zp1} being 17·6 times larger than in the previous case. Though vapour bubbles differ substantially from the gas bubbles, to a first approximation they can be modelled by gas bubbles having sufficiently large amplitudes of oscillations [2]. Then using the scaling function p_{zp} (fig. 5) we find that for $p_{zp1} = 167$ and $\gamma = 1{\cdot}33$ the corresponding amplitude is $A_1 \doteq 3{\cdot}5$, and for $p_{zp1} = 167$ and $\gamma = 1{\cdot}25$ the amplitude is $A_1 \doteq 3{\cdot}29$. These values are much larger than those found in the case of the explosion generated bubbles.

It may also be interesting to estimate the value of the maximum pressure, P_{M1}, in the two examples. Let us assume that the actual amplitude, A_1, is determined by the value of the peak pressure, p_{zp1}. In the case of the underwater explosions we have found that for $p_{zp1} = 9{\cdot}5$ and $\gamma = 1{\cdot}25$ the amplitude is $A_1 = 2{\cdot}05$. Then from fig. 10 it follows that $Z_{m1} = 0{\cdot}16$ and hence $P^*_{M1} = (A_1 Z_{m1})^{-3\gamma} = 65{\cdot}4$. As the ambient pressure is $p_\infty = 1{\cdot}62$ MPa, we finally obtain the result that $P_{M1} = 106$ MPa.

In the case of the spark bubbles we have determined that $p_{zp1} = 167$ and hence for $\gamma = 1{\cdot}33$ we have $A_1 \doteq 3{\cdot}5$. Then $Z_{m1} = 0{\cdot}034$ and $P^*_{M1} = 2871$. As $p_\infty = 100$ kPa in this case, we finally have that $P_{M1} = 287{\cdot}1$ MPa. Note the interesting result that although p_{zp1} in the two examples differs by a factor of 17·6, the maximum pressure P_{M1} differs only by a factor of 2·76. This result is to be attributed, evidently, to the difference in the ambient pressures, p_∞.

6. BUBBLE PULSE SPECTRUM

Knowledge of the bubble pulse spectrum is useful, for example, in determining the optimum bandwidth of the measuring experimental apparatus. In this section we shall give two approximate formulae that can be conveniently used for this purpose. The formulae are based on the scaling functions T_{zc} and ϑ_z.

In the case of the underwater explosions the bubble pulse spectrum was studied both experimentally and theoretically by Weston [15]. It was found that the spectrum is approximately flat between frequencies f_l and f_u. Below and above these frequencies the spectrum falls off at 6 dB/octave. A similar situation can also be expected in the case of other excitation techniques. Thus the required bandwidth of the measuring apparatus (hydrophones, amplifiers, etc.) should extend at least from f_l to f_u, and if possible, should be broader.

The frequencies f_l and f_u can be determined from the following approximate formulae:

$$f_l = \frac{1}{T_{01}} = \frac{1}{2R_{M1}T_{zc1}(\varrho_\infty/p_\infty)^{1/2}}, \tag{41}$$

$$f_u = \frac{1}{2\pi\vartheta_1} = \frac{1}{2\pi R_{M1}\vartheta_{z1}(\varrho_\infty/p_\infty)^{1/2}}. \tag{42}$$

For water under ordinary laboratory conditions it holds that $(\varrho_\infty/p_\infty)^{1/2} \doteq 0{\cdot}1$ and the values of T_{zc1} and ϑ_{z1} can be determined from figs. 4 and 6.

As a concrete example let us consider two bubbles oscillating with an amplitude $A_1 = 3{\cdot}5$ and having sizes $R_{M1} = 1$ mm in the first case and $R_{M1} = 10$ mm in the second case. Assuming $\gamma = 1{\cdot}33$ we can find out from figs. 4 and 6 that $T_{zc1} \doteq 0{\cdot}92$ and $\vartheta_{z1} \doteq 10^{-3}$, respectively. Then for $R_{M1} = 1$ mm we obtain from eq. (41) that $f_l = 5{\cdot}5$ kHz and from eq. (42) that $f_u = 1{\cdot}6$ MHz. Similarly, for $R_{M1} = 10$ mm we have $f_l = 550$ Hz and $f_u = 160$ kHz. Hence, whereas in the case of the larger bubble suitable commercial hydrophones are available, in the case of the small bubble we need a hydrophone of a special design, which may often be a problem.

As a second example let us examine how the required bandwidth varies with the amplitude of the bubble oscillations. Let us now consider three bubbles of equal size $R_{M1} = 10$ mm and having the same adiabatic exponent $\gamma = 1{\cdot}33$. Let the first bubble oscillate linearly with the amplitude $A_1 = 1{\cdot}01$, the second with the amplitude $A_1 = 2$ (the gas bubble) and finally the third bubble with the amplitude $A_1 = 3{\cdot}5$ (the vapour bubble). The corresponding bandwidths are: $f_l \doteq f_u \doteq 318$ Hz in the first case; $f_l = 500$ Hz and $f_u = 5{\cdot}3$ kHz in the second case; and finally $f_l = 550$ Hz and $f_u = 160$ kHz in the third case.

7. CONCLUSION

The method of the scaling and independent functions makes it possible to confront the theoretical model with experimental data. When evaluating the data obtained in experiments with explosion generated bubbles, a serious discrepancy between the theory and experiment was revealed. Unfortunately, as no similar experimental data are available for other bubbles, it cannot be verified at present, whether this discrepancy is a particular feature of the explosions or a general one valid for all bubbles. Especially puzzling is the finding that the unaccounted energy loss (i.e. $\Delta E_d - \Delta E'_a$) is very large even in the case of the second bubble pulse, when the amplitude of the bubble oscillation is relatively small.

The computed scaling and independent functions can be applied directly to scaling gas bubbles. Some caution, however, is necessary, when interpreting data originating from vapour or non-scaling gas bubbles.

It seems that to solve the bubble dynamics mystery, a combined use of as many measuring methods as possible will be necessary. For example, high-speed cinematography alone, though very important in monitoring the bubble size, shape, and translational motion, can provide only a limited amount of information. This information concerns, for example, the maximum bubble radii in the successive bubble oscillations. From these data the damping factor can easily be determined. But, as shown in section 5, this is not sufficient for assessing the bubble oscillation intensity eorrectly, because the use of the damping factor alone leads to exaggerated amplitude cstimates.

Hence, further methods, including non-traditional ones, are highly desirable. In this respect, recent progress in the high-speed holocinematography [16–18] represents a step forward and should enable us to gain a better understanding of the complicated phenomena associated with the violent bubble oscillations.

8. CORRECTIONS

The author would like to correct a few statements given in the previous papers [1, 3]. First, the earliest derivation of eq. (I-12) is due to Besant [19] and not to Rayleigh [20] as stated in the introduction to the paper [1]. Though Rayleigh himself mentiones Besant's result, this was until recently not easily accessible. It is Hammitt's merit that Besant's original analysis was reprinted [21] and thus made available.

Second, an exact solution of eq. (I-12) has been obtained for the particular case of $\gamma = 4/3$ by Childs [22] in terms of elliptic integrals.

Third, energy dissipation due to viscosity (integral (III-23)) was given first by Taylor [23] and this was nine years before Poritsky [24] to whom the analysis of the viscosity effects is nowadays generally ascribed.

Finally, in evaluating integral (I-23) only the first two terms from the right-hand side of eq. (I-21), i.e. the acoustic field, should be used. This may be not so obvious from the notation used in [1].

Received 7. 5. 1985.

References

[1] Vokurka K.: Czech. J. Phys. B *35* (1985) 28.
[2] Vokurka K.: Czech. J. Phys. B *35* (1985) 110.
[3] Vokurka K.: Czech. J. Phys. B *35* (1985) 121.
[4] Vokurka K.: Acustica *59* (1986) 214.
[5] Vokurka K.: Acustica *60* (1986) (to appear).
[6] Vokurka K.: J. Sound and Vib. *105* (1986) (to appear).
[7] Cole R. H.: Underwater Explosions, Princeton University Press, Princeton, 1948.
[8] Arons A. B., Yennie D. R.: Rev. Mod. Phys. *20* (1948) 519.
[9] Arons A. B., Slifko J. P., Carter A.: J. Acoust. Soc. Am. *20* (1948) 271.
[10] Lauterborn W.: Acustica *31* (1974) 51.
[11] Vokurka K.: Acta Tech. ČSAV *30* (1985) 585.
[12] Minnaert M.: Philos. Mag. *16*, Ser. 7 (1933) 235.
[13] Crum L. A.: J. Acoust. Soc. Am. *73* (1983) 116.
[14] Mellen R. H.: J. Acoust. Soc. Am. *28* (1956) 447.
[15] Weston D. E.: Proc. Phys. Soc. (London) *76* (1960) 233.
[16] Kuhnke K.: Ph. D. Dissertation, University of Göttingen, Göttingen, 1979 (in German).
[17] Merboldt K. D., Lauterborn W.: Opt. Commun. *41* (1982) 233.
[18] Lauterborn W., Vogel A.: Annu. Rev. Fluid Mech. *16* (1984) 223.
[19] Besant W. H.: A Treatise on Hydrodynamics. Cambridge University Press, Cambridge, 1859.
[20] Rayleigh J. W.: Philos. Mag. *34*, Ser. 6 (1917) 94.
[21] Hammitt F. G.: Cavitation and Multiphase Flow Phenomena, McGraw-Hill, New York, 1980.
[22] Childs D. R.: Int. J. Non-Linear Mech. *8* (1973) 371.
[23] Taylor G. I., Davies R. M.: *in* The Scientific Papers of Sir. G. I. Taylor, Vol. III, (ed. G. K. Batchelor), Cambridge University Press, Cambridge, 1963, p. 337.
[24] Poritsky H.: *in* Proc. 1st U.S. National Congress on Appl. Mech., (ed. E. Sternberg), New York, 1952, p. 813.
[25] Vokurka K.: Ph. D. Dissertation, Czech Technical University, Prague, 1979 (in Czech).
[26] Vokurka K.: *in* Cavitation Research II, ČSVTS, Prague, 1979, p. 23 (in Czech).